

Loss engineering of a bimodal waveguide platform for biosensing

Student paper

Samuel M. Hörmann^{1,2,*}, Jakob W. Hinum-Wagner^{1,2}, Gandolf Feigl², Alexander Bergmann²

¹ ams-OSRAM AG, Tobelbader Straße 30, 8141 Unterpremstätten, Austria

² Institute of Electrical Measurement and Sensor Systems, Graz University of Technology, Inffeldgasse 33/I, 8010 Graz, Austria

* samuel.hoermann@ams-osram.com

An advantageous implementation of an integrated photonic biosensor is the bimodal waveguide interferometer. To fully utilize its potential and minimize the limit of detection, it is essential to holistically design its waveguide platform. To this end, we incorporate an ab initio model of the surface-roughness-induced scattering to find a balance between predicted sensitivity and losses for a silicon nitride strip waveguide platform.

Keywords: Bimodal, biosensor, scattering, surface roughness, silicon photonics, silicon nitride

INTRODUCTION

Point-of-care devices are poised to revolutionize the healthcare sector [1]. Integrated photonic biosensors are seamlessly integratable into CMOS fabs and thus can be reliably produced at ultra-large scale [2]. Typically, they rely on transducing the refractive index change induced by binding events between the analyte and bioreceptors. To this end, the bioreceptors are immobilized on a waveguide that facilitates the interaction of the guided light and the bioreceptor-analyte-complex in the solution flown around the waveguide. Their limit of detection (LOD) can be in the femto- and attomolar range [1]. Thus, they are ideal to contribute to this revolution in personal medicine and rapid diagnostics, where precision and manufacturability are vital. However, this technology can only fully utilize its potential, if the integrated photonics is holistically designed. Often, only the sensitivity is maximized while the losses are neglected. To minimize the LOD, however, a balance needs to be found between these two parameters. For that purpose, we utilize a recently developed model [3] of the surface-roughness-induced scattering to incorporate the scattering losses into the design of a bimodal waveguide platform (see Fig. 1). This model is based on the volume current method and allows the ab initio calculation of the scattering loss coefficient for a given waveguide's mode and surface roughness autocorrelation.

RESULTS

Using silicon nitride as the waveguide's core material is beneficial in many ways: First and foremost, it is transparent in the visible to near-infrared wavelength range which overlaps with the therapeutic window. Secondly, it has a lower refractive-index contrast leading to lower surface-roughness-induced scattering losses. Finally, it may be deposited monolithically in CMOS fabs [4]. For these reasons, we consider a silicon nitride waveguide platform based on strip waveguides (as in Fig. 1 and Fig. 2).

In a previous analysis, we investigated different forms of the surface roughness' autocorrelation for their descriptive power [5]. We discovered that a kernel of the Matérn class is beneficial over the established exponential kernel. Furthermore, within the scattering model exhibits the degree of anisotropy of the autocorrelation shows a significant impact on the scattering coefficient. Moreover, conflicting evidence regarding the assumption of perfect vertical striations can be found in microscope images of the sidewall roughness [6], [7] and in a previous evaluation of the anisotropy [8]. Hence, we base our calculations on a two-dimensional, anisotropic Matérn 3/2 kernel κ with finite correlation lengths l_y and l_z , which are along the waveguide height and length, resp. (see Fig. 2). This reads

$$\kappa(y, z) = \sigma^2 \left(1 + \frac{\sqrt{3}y}{l_y}\right) \left(1 + \frac{\sqrt{3}z}{l_z}\right) e^{-\sqrt{3}\left(\frac{y}{l_y} + \frac{z}{l_z}\right)} \quad (1)$$

with the surface roughness' standard deviation σ [9]. For the calculations, we also need the spectrum of the z-component, which can be calculated via the Fourier transform [3].

In an integrated, refractometric biosensor each mode's propagation coefficient β has a sensitivity S per waveguide length to a homogeneous change in the relative permittivity ε_p in a subsection A of the waveguide cross-section described by

$$S = \frac{\partial \beta}{\partial \varepsilon_p} = \frac{\varepsilon_0 \omega}{4P} \int_A \|\vec{E}(x, y)\|^2 dx dy \quad (2)$$

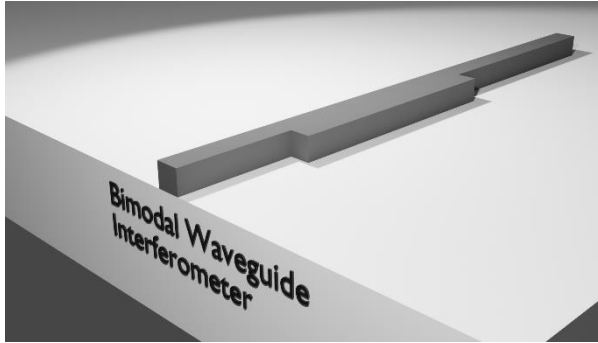


Fig. 1. Sketch of a bimodal waveguide interferometer based on strip waveguides with a vertical step junction.

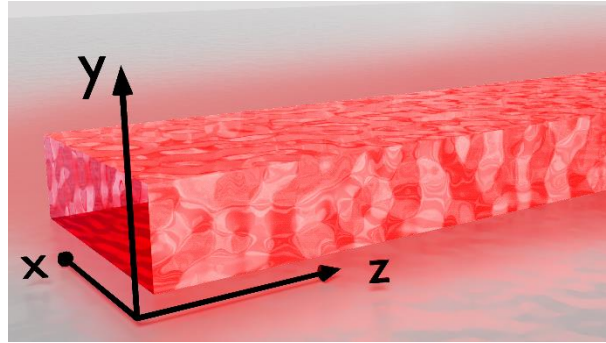


Fig. 2. Stylized image of surface-roughness-induced scattering. Taken from [3].

where $\vec{E}(x, y)$ is the mode's electric field and P is its power [10]. In a bimodal waveguide interferometer, the relevant parameter is the difference of the two modes' sensitivity $S = |S_1 - S_2|$ in the bimodal section. Rather than the sensitivity difference, however, the sensitivity difference over the sum of the loss coefficients is our figure of merit (FOM), since it determines the maximum slope of the spectral interference pattern:

$$FOM = \frac{|S_1 - S_2|}{\alpha_1 + \alpha_2} \quad (3)$$

That is because, lower losses allow for a longer optimal length of the bimodal section, which evaluates to $(\alpha_1 + \alpha_2)^{-1}$, causing higher total sensitivity achievable with the platform. We consider only the sidewall-roughness-induced scattering, since this is the primary loss contributor in silicon photonics.

The sidewall roughness' parameters were evaluated from AFM measurements of the sidewall of a corresponding fabricated integrated photonic system. The deposition and measurement techniques will be discussed in more detail in a following publication. According to the above-stated framework, we used HDP CVD to deposit the silicon oxide layer on top of a silicon substrate. To structure the silicon nitride waveguide core, LPCVD with DUV and reactive ion etching was utilized. The system was not cladded, to enable the interaction of the modes with the sensing medium and to retain access to the sidewalls for the AFM measurements. The surface roughness' parameters are characteristic of the fabrication process and ideally irrespective of the silicon photonic layout. The best fitting parameters of the Matérn kernel for this fabrication process are: $\sigma = 2.2$ nm, $l_z = 82$ nm, $l_y = 68$ nm.

We compute the waveguide's modes in Ansys Lumerical (version: 2022 R1, module: MODE, solver: Finite Difference Eigenmode (FDE)). Using the above formulae, we can calculate the predicted sensitivity, the scattering losses, and FOM for each combination of width and height. By definition, the parameter space of the bimodal system is limited by the necessity to have exactly two modes of the same polarization. Further, we set the wavelength to 850 nm and we used the refractive indices: $n_{SiN} = 1.9$, $n_{silica} = 1.455$, and $n_{water} = 1.325$. As an additional restriction, we consider only transverse-electric-like (TE) modes.

The resulting sensitivity to refractive index changes in the cladding (in our case the water over the waveguide system) per unit length is depicted in Fig. 3. We recognize that there is a maximum at low widths and high heights of the waveguide. Hence, higher waveguides have increased interaction with the vicinity. This is caused by the higher intensity of the TE-like modes at the sides of the waveguide. However, the more impactful FOM shows its maximum at high widths and low heights. This disparity illustrates the importance of the holistic approach. Moreover, we recognize that there is approximately a factor of two between the best and worst platform design, as predicted by the above model.

DISCUSSION

An important circumstance that should be considered for the implementation of the waveguide platform in actual structures is that the FOM from eq. (3) and Fig. 4 is proportional to the slope of the spectral interference at the inflection point, but only if the length of the bimodal section equals the optimal $(\alpha_1 + \alpha_2)^{-1}$. For the configuration with a height of 200 nm and a width of 1200 nm, this evaluates to 111 μ m. That is one to two orders of magnitudes higher than typically used interferometric structures [1], [2]. Naturally, the longer the sensing structure, the more area it will occupy on the die and the higher the costs. If another length is fabricated, the actual length needs to be used instead in eq. (3), which reduces the scattering's impact and increases the importance of high sensitivity.

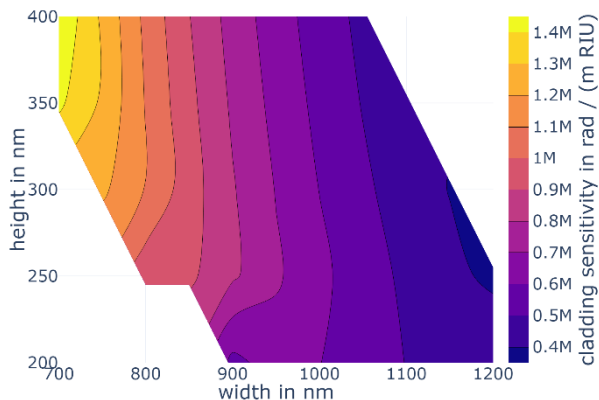


Fig. 3. Sensitivity per unit length of the bimodal waveguide platform operated in the TE-like mode at a wavelength of 850 nm to refractive index changes in its cladding.

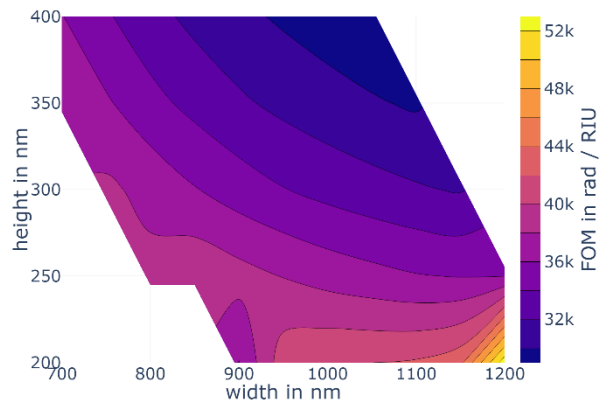


Fig. 4. FOM of the bimodal waveguide platform operated in the TE-like mode at a wavelength of 850 nm for refractive index sensing.

Finally, we want to stress that real fabrication conditions will lead to non-ideal waveguides. Real waveguides will have sloped sidewalls leading to deformed electric field profiles and subsequently to different sensitivity and losses. Hence, the above predictions will only be valid if the process parameters are adjusted well enough such that the simulated modes tolerably represent the real ones.

CONCLUSION

We saw above that a holistic approach, which includes surface-roughness-induced scattering, drastically changes the design choices for the bimodal waveguide platform of a refractometric biosensor. For an optimal sensing performance of a bimodal waveguide interferometer fabricated within the above parameters, a bimodal section with a low height and high width is predicted to be advantageous. Furthermore, we notice the advantage this scattering model has in being able to directly calculate the losses from the surface roughness' parameter and the modes. To the best of our knowledge, the anisotropic Matérn kernel with finite correlation lengths was also applied for the first time in the context of surface-roughness-induced scattering. As mentioned above, this autocorrelation function is expected to better capture the statistical characteristics than the commonly applied exponential kernel, as analyzed in [5]. That is because, the latter leads to non-continuously differentiable sample functions, whereas the former is one time continuously differentiable.

References

- [1] M. Soler, M. C. Estev, M. Cardenosa-Rubio, A. Astua, L. M. Lechuga, *How Nanophotonic Label-Free Biosensors Can Contribute to Rapid and Massive Diagnostics of Respiratory Virus Infections: COVID-19 Case*, ACL Sensors, vol. 5, no. 9, 2020
- [2] L. Chrostowski, M. Hochberg, *Silicon photonics design*, Cambridge University Press, 2015
- [3] S. M. Hörmann, J. W. Hinum-Wagner, A. Bergmann, *An Ab Initio, Fully Coherent, Semi-Analytical Model of Surface-Roughness-Induced Scattering*, Journal of Lightwave Technology, 10.1109/JLT.2022.3224777, 2022
- [4] D. J. Blumenthal, R. Heideman, D. Geuzebroek, A. Leinse, C. Roeloffzen, *Silicon Nitride in Silicon Photonics*, in Proceedings of the IEEE 106.12, pp. 2209-2231, 2018
- [5] S. Hörmann, J. W. Hinum-Wagner, J. Sattelkow, D. Rist, A. Bergmann, *Comparison of Gaussian Process Kernels for Surface Roughness Modelling*, in Proceedings of the 23rd European Conference on Integrated Optics, pp. 57-59, 2022
- [6] C. G. Poulton, C. Koos, M. Fujii, A. Pfrang, T. Schimmel, J. Leuthold, W. Freude, *Radiation modes and roughness loss in high index-contrast waveguides*, IEEE Journal of selected topics in quantum electronics, vol. 12, no. 6, 2006
- [7] J. H. Jang, W. Zhao, J. W. Bae, D. Selvanathan, S. L. Rommel, I. Adesida, A. Lepore, M. Kwakernaak, J. H. Abeles, *Direct measurement of nanoscale sidewall roughness of optical waveguides using an atomic force microscope*, Applied physics letters, vol. 83, no. 20, 2003
- [8] E. Jaberansary, T. M. Masaud, M. M. Milosevic, M. Nedeljkovi, G. Z. Mashanovich, H. M. Chong, *Scattering loss estimation using 2-D Fourier analysis and modeling of sidewall roughness on optical waveguides*, IEEE Photonics Journal, vol. 8, no. 5, 2013
- [9] C. E. Rasmussen, C. K. I. Williams, *Gaussian Processes for Machine Learning*, MIT Press, 2005
- [10] J. Milvich, D. Kohler, W. Freude, C. Koos, *Surface sensing with integrated optical waveguides: a design guideline*, Optics express, vol. 26, no. 16, 2018